

Research on the Adaptability of Packers for Integrated String Fracturing Operations in Low Porosity and Low Permeability Reservoirs

Zhiyong Wan^{1,*} – Hao Yu¹ – Yong Xiao² – Zhaoyang Zhao¹ – Zhanghua Lian¹ – Fangxin Chen¹

¹ Southwest Petroleum University, State Key Laboratory of Oil and Gas Reservoir Geology and Exploitation, China

² Chengdu North Petroleum Exploration and Development Technology Co, Ltd, China

To study the failure of conventional packers in the fracturing and stimulation of low-porosity and low-permeability reservoirs and reduce the failure accidents of packers in the fracturing process, a suitable integrated string packers was selected in the process of fracturing and stimulation in an oilfield in the Middle East as a case study. Three different well types have been established. The wellbore temperature distribution and the axial force of the string can be calculated under the conditions of various wellhead pressures and different displacement, and it is found that the temperature at the bottom of the well can reach 130 °C, and the maximum axial force at the wellhead is 500 kN. At the same time, the applicability of retrievable tubing testing squeeze (RTTS) and hydraulic-set retrievable (RH) packer in different working conditions was evaluated, and it was found that only RTTS packers can meet the needs of the oil field. According to the calculated temperature field and axial force distribution, the stress on different components of the packer under different working conditions is established during the fracturing-stimulation operation. In the worst working conditions, the maximum stress of the packer occurs at the lower part of the central pipe, reaching 303.83 MPa, which is in a safe state. The contact stress on rubber rings can reach 30 MPa, indicating that the sealing performance can meet the requirements of on-site use. The temperature and axial force data calculated by the model provide a theoretical basis for safe well control. At the same time, through model evaluation, it was found that the RTTS packer can be suitable for the fracturing and stimulation needs of the oilfield. The research methods and achievements in the article provide theoretical guidance for evaluating the applicability of packers in the fracturing and stimulation process of low porosity and low permeability reservoirs.

Keywords: low porosity and low permeability reservoirs, integrated pipe string, packer rubber ring, acid fracturing, finite element simulation

Highlights

- Established a practical applicability evaluation model for three types of well types used in a Middle Eastern oil field.
- Based on the results obtained from the adaptability evaluation model of the packer, combined with the finite element method to calculate the stress distribution of key components on the packer, it is found that the upper central pipe of the packer is a weak structure.
- Combined with the contact pressure and contact length obtained by finite element calculation, the sealing performance of the rubber ring under extreme conditions was evaluated, and the adaptability evaluation model of the rubber ring of the packer was established.

0 INTRODUCTION

In recent years, with the improvement of mining technology, more low-porosity and low-permeability reservoirs have been developed. In order to activate the reservoir and increase production, it is necessary to use acid fracturing technology [1]. However, the reservoir is characterized by high crustal stress, easy leakage, interlayer interaction, strong formation heterogeneity, relatively developed fractures, and great difficulty in oil testing and reservoir reconstruction. The conventional operation of lowering the string multiple times cannot meet the requirements of oil and gas well testing and acidizing stimulation operations [2]. Therefore, in the process of acid fracturing operation, the perforation-fracturing-completion triple integrated string operation is adopted, which

has reliable tool function and stable performance, reducing the number of frequently lowered strings and damage to the reservoir [3]. It can also improve construction efficiency, save the cost of exploration and development, avoid the secondary pollution of the formation by the well control fluid to the greatest extent, meet the needs of environmental protection, fracturing displacement and efficient construction [4], and can solve the problem of out-of-control wellhead during the installation of blowout preventers, to reduce well control risks, construction risks and operating costs [5]. To realize the perforation-fracturing-completion operations once, the design of the integrated string is more stringent. There are still defects, such as insufficient understanding in the design, which seriously restricts the development of

special reservoir characteristics, such as low porosity and low permeability [6] and [7].

At present, the research on the design of the integrated string mainly focuses on the research on the failure of the thread seal [8] and [9], the construction process of the integrated operation string [10], and the design of the perforation-pressure test dual string. For harsh reservoir conditions, such as low porosity and low permeability, research on the use of perforating-fracturing-completion triple-integrated operation strings is lacking. In conventional production operations, the string is often run in three times, which increases the risk of reservoir damage, and the wellhead needs to be lifted and lowered multiple times, which increases the risk of well control failure. Compared with the integrated operation string, the construction operation time is increased, as are the development costs of oil and gas reservoirs [11]. Therefore, this article focuses on three different well types developed in a Middle Eastern oil field with low porosity and low permeability reservoirs, namely vertical wells, deviated wells, and horizontal wells. Key components in the integrated perforation fracturing completion operation string used for special reservoir development include a numerical simulation model for wellbore string temperature and axial force during perforation and fracturing processes, as well as an evaluation model for the applicability of packers, which was established through software. The simulated temperature and axial force data were then combined with finite element analysis software. Conduct applicability analysis and research on key components of integrated operation string, provide theoretical basis and guidance for the failure research of key components of integrated operation string used in oil fields, and also provide theoretical basis for the design of integrated operation string and various safe construction operations.

1 INTEGRATED PIPE STRING STRUCTURE AND ANALYSIS OF ITS STRESS CONDITIONS

1.1 Structure and Working Principle of Key Components of Integrated Pipe String

At present, in the development process of some oil and gas fields, multiple lowering pipe strings are used [12]. The schematic diagram of the operation process is shown in Fig. 1.

First, the well-cleaning and scraping strings are lowered to clean the debris attached to the inner wall of the strings, and then the perforated strings are lowered for perforation operations, and finally

the acid fracturing and well completion operations are performed. During this series of operations, it is necessary to open the wellhead several times to raise and lower the pipe string, increasing the risk of well control failure, but the integrated operation string can prevent it. Therefore, an oilfield in the Middle East actually uses the perforation-fracturing-completion triple integrated operation string, which consists of tubing, rupture disk (RD) cycle valve, rupture disk safety (RDS) valve, OMNI™ valve, packer, tubing conveyed perforation (TCP) gun and other components. The three different wellbore structures and integrated pipe strings used are shown in Fig. 2.

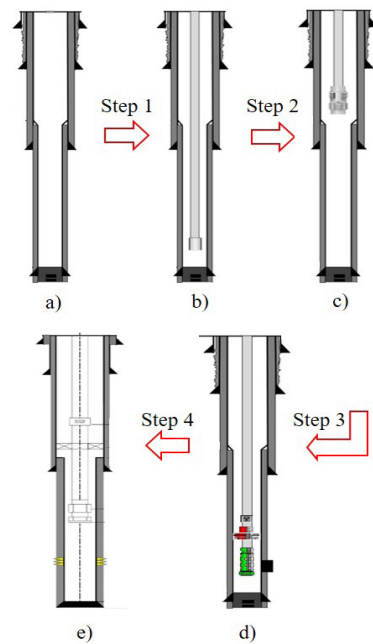


Fig. 1. Schematic diagram of the operation process of repeatedly lowering the pipe column; a) hole structure, b) wiper string, c) scraper string, d) perforation string, and e) completion string

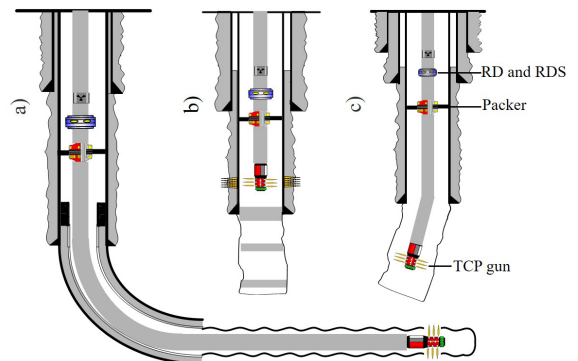


Fig. 2. Schematic diagram of three types of wellbore structures and integrated pipe string structures; a) horizontal well, b) vertical well, and c) deviated well

As a key component of the integrated string, the packer determines the sealing performance of the operating string during perforation and acid fracturing; therefore, an in-depth safety analysis is required. There are two packer selection schemes on site: the RTTS packer and the RH packer. The technical parameters and manufacturer of the packer are shown in Table 1. The structural schematic diagrams of the two packers are shown in Fig. 3.

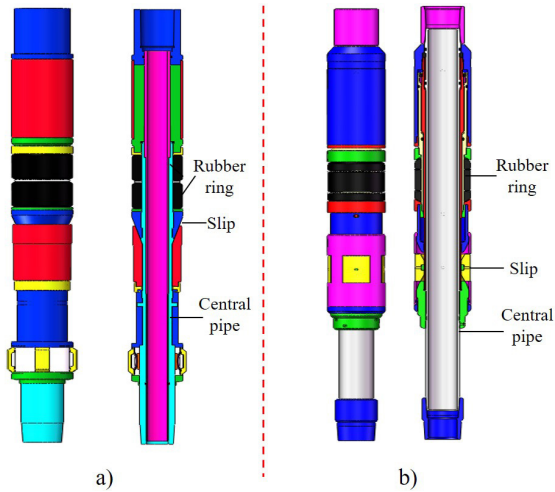


Fig. 3. Structural schematic diagram of; a) RTTS packer, and b) RH packer

The RTTS packer is a suspension packer with a large diameter and can seal off two-way pressure. It consists of a slot transposition mechanism, slips, rubber ring and hydraulic anchoring mechanism. The hydraulic anchoring mechanism can prevent the lower part of the packer from being pushed out of the wellbore when the pressure is too high. It is also equipped with friction blocks and an automatic groove sleeve structure. Designed for formation testing, acidizing, and cementing plug well operations, the large diameter is used to pump a large amount of fluid under a small pressure drop and can pass through the tubing perforating gun. Its working principle is that when it is necessary to seal the annular space between the tubing and the production casing, the upper limit groove of the packer is rotated so that the upper structure of the packer can move axially within the

allowable range of the limit. When the string applies a part of its own weight and axial displacement to the RTTS packer, the slips are stretched to fix the packer on the inner wall of the production casing, and then continue to apply its own weight and axial displacement until the rubber ring of the packer is fully supported and the annulus between the oil pipe and the production casing is completely sealed.

The other type of packer planned to be selected on site is the hydraulic retrievable packer, which is a compact, sturdy, reliable, convenient to use, single column hydraulic retrievable packer that can be directly lifted up and released. It is suitable for applications such as deviated wells, multi packer completion. The envelope curves for the sealing performance of two types of packers are shown in Fig. 4.

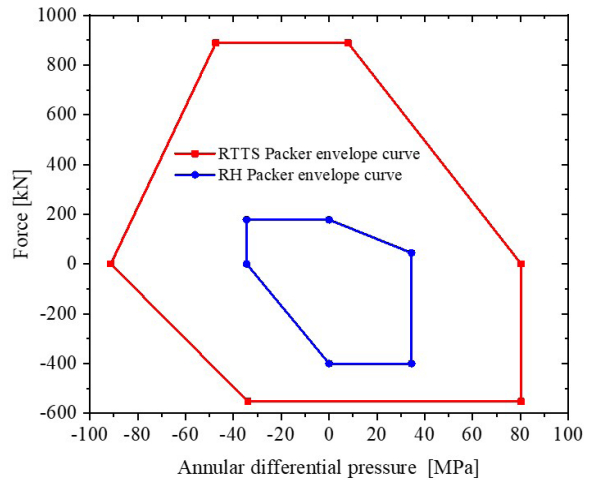


Fig. 4. Envelope Curve of RTTS Packer and RH Packer

The packing capacity of the two packers selected on site can be obtained from Fig. 4. The red shape in the figure is the envelope curve of the RTTS packer, while the envelope curve of the RH packer is the blue shape, and the envelope of the RTTS packer completely encompasses the RH packer, indicating that the packing ability of the RTTS packer is better than that of the RH packer.

Table 1. Manufacturer and technical characteristics of the packers

Packer type	Maximum outer diameter [mm]	Minimum inner diameter [mm]	Length [mm]	Working pressure [MPa]	Working temperature [°C]	Applicable tubing diameter [mm]	Manufacturer
RTTS	201	124	1450	25 to 100	20 to 150	177.8	GWDC
RH	213	137	1300	10 to 60	20 to 120	177.8	TechWest

1.2 Theoretical Analysis of the Failure of Key Components of Packers

As an important part of ensuring the sealing ability of the packer, the packer rubber ring needs to be analysed thoroughly. The rubber ring is made of rubber, which is a typical hyper-elastic body.[13] and [14] It is often described with the Mooney-Rivlin constitutive model, and its constitutive relation expression is:

$$W = C_{10}(I_1 - 3) + C_{01}(I_2 - 3), \quad (1)$$

where W is the density of strain energy [J/m³], C_{10} and C_{01} are the Mooney-Rivlin coefficients of the material [MPa], and I_1 and I_2 are the first and second strain tensor invariant, [1].

The relationship between shear modulus and elastic modulus is:

$$\begin{cases} E = 6(C_{10} + C_{01}) \\ G = 2(C_{10} + C_{01}) \end{cases} \quad (2)$$

According to the large deformation properties of rubber, the relationship between its elastic modulus E , shear modulus G and material constants is:

$$\begin{cases} E = 6(C_{10} + C_{01}) \\ G = 2(C_{10} + C_{01}) \end{cases} \quad (3)$$

According to the rubber compression test, due to $E = 11.49$ MPa, the simulation results are relatively close to the measured results, resulting in $C_{10} = 1.879$ MPa and $C_{01} = 0.038$ MPa.

In acid fracturing operations, the fracturing fluid injected from the wellhead is regarded as a Newtonian fluid, and when it flows to the target layer, the calculation formula for pipe flow friction is:

$$R_e = \frac{\rho v_i d}{\mu}, \quad (4)$$

where R_e is the pipe flow friction; ρ is the fluid density [kg/m³], v_i the fluid velocity, [m/s], d the inner diameter of the pipe column [m], and μ the fluid viscosity, [kg/(s·m)].

When the Reynolds number R_e of the acid fluid in the wellbore is less than 2000, the flow state of the acid fluid in the wellbore is a laminar flow state. At this time, the hydraulic friction coefficient of the fracturing fluid in the wellbore in the pipeline is [15]:

$$f = \frac{64}{R_e}. \quad (5)$$

When the Reynolds number R_e of the acid fluid in the wellbore is greater or equal to 2000, it is in a turbulent state. At this time, the hydraulic friction

coefficient of the fracturing fluid in the wellbore in the pipeline is:

$$f = \frac{0.079}{R_e^{0.25}}. \quad (6)$$

However, when the fluid flows to the bottom of the well in the annular space, it will be subjected to friction along the way to reduce the pump pressure. The formula for calculating the friction loss of the fluid along the way is:

$$\Delta P = f \frac{\rho L v_i^2}{2gd}, \quad (7)$$

where ΔP is the frictional loss along the way [kg/m²], L is the length of the pipeline along the route [m], and g is the gravitational acceleration [m/s²].

When the fluid reaches the bottom of the well, since the temperature of the injected fluid at the wellhead is much lower than the temperature of the downhole formation, the temperature of the wellbore will change during the acid fracturing operation, resulting in thermal expansion and contraction.

The temperature effect expression is [16]:

$$\varepsilon_T = \alpha \cdot \Delta T, \quad (8)$$

where ε_T is the thermal expansion elongation per unit length [m/m = 1], the expansion coefficient [m/°C] and ΔT the temperature difference [°C].

In the process of acid fracturing, it is often necessary to suppress the pressure of the wellbore, and the pressure mainly acts on the inner wall of the string, which will cause the axial deformation of the string. At the same time, in order to protect the downhole tools, such as packers, from failure, it is necessary to apply pressure to the annulus by squeezing the string from outside to inside will result in a reduction in the diameter of the string and an axial elongation.

The pressure inside the tubing consists of two parts: pump pressure and the hydrostatic column pressure of the liquid inside the tubing.

$$P_i = P_p + \rho_i g h, \quad (9)$$

where P_i is the pressure inside the tubing [MPa], P_p is the surface pump pressure [MPa], and ρ_i the fluid density inside the casing [kg/m³].

The external pressure of the pipeline is mainly the static liquid column pressure of the annular liquid, which is $P_o = \rho_o g h$, where ρ_o is the density of liquid in the annular space [17] and [18].

The total axial deformation of the oil pipe under the combined action of internal and external pressures is:

$$\Delta l = -\int_0^H \frac{2\nu}{E} \cdot \frac{P_o R^2 - P_i}{R^2 - 1} dh, \quad (10)$$

where d_o is the outer diameter of the oil pipe [m], d_i the inner diameter of the oil pipe [m] where $R = d_o / d_i$, H the depth of pipe string [m], and ν Poisson's ratio.

When the axial load on the string in the wellbore exceeds a certain critical value, the string will lose its stable state and buckle, causing the string to shrink, shorten, bend, and deform, and increase the friction between the string and the wellbore. The axial deformation of the packer will cause the seal failure of the packer and even the plastic failure of the string.

Then the true axial force of the tubing cross section at any well depth is F_a , and the equivalent axial force F_e is:

$$F_e = F_a + P_o A_o - P_i A_i, \quad (11)$$

where A_o is the outer circular area of the column cross-section [mm²], and A_i is the internal circular area of the pipe column cross-section [mm²].

The critical value of helical buckling deformation of the pipe column is [19]:

$$F_{hel} = 5.55\sqrt[3]{EIq_m^2}, \quad (12)$$

where F_{hel} is the critical buckling load [kN], q_m is the line floating weight of the oil pipe [kN/m] and EI is the bending stiffness of the oil pipe [kN·m²].

When the pipe column is in a helical buckling state, the bending stress on the pipe column σ_m is:

$$\sigma_m = \frac{M}{W} = \frac{2Fr_{out}^2}{\pi(r_{out}^4 - r_{in}^4)}, \quad (13)$$

where σ_m is the bending stress when the pipe string undergoes helical buckling [MPa], M is the bending moment at the central pipe when the pipe column undergoes helical buckling [N/mm], and W is the bending section coefficient of a circular section [mm³].

By calculating the stress on the string and comparing it with the yield strength of its material, if it is less than the yield strength, it means that the pipe string is still in a safe state. Although the average

stress on the integrated pipe string can be evaluated and calculated by Eq. (13), the pipe string is not regular, and it is impossible to accurately calculate the force on the upper part of the packer with an analytical formula, and only the finite element method can be used for simulation.

2 TEMPERATURE AND AXIAL FORCE ANALYSIS OF INTEGRATED PIPE STRING

According to the data provided by the Halfaya Oilfield in Iraq [20], the average porosity of the B1, B2, and B3 sub-member of the Sadi Formation is 17.5 %, 19.3 %, and 13.6 %, respectively, and the average permeability is 0.13 mD, 0.2 9 mD, and 5.11 mD, respectively. It belongs to a low porosity, ultra-low permeability carbonate reservoir, with a wellbore temperature of 25 °C, a fracturing fluid density of 1200 kg/m³, a wellhead injection pressure of 30 MPa to 50 MPa, and a displacement of 3 m³/min to 5 m³/min. The data on the wellbore structure and the integrated string structure used are summarized in Table 2, The geological structure of the Halfaya Oilfield is shown in Fig. 5.

X1 to X3 wells are three typical well types developed in an oil field in Middle East. The obtained data were used to establish an integrated string temperature and axial force analysis model using software, and the temperature, axial force, axial safety factor, and packer applicability were calculated for different layers of the wellbore structure.

2.1 Analysis of Temperature Field Calculation Results for Integrated Pipe String

Since the higher the wellhead pumping pressure and displacement, the larger the volume of the pumped fluid, the more intense the downhole string cooling, so the analysis and calculation of the temperature of the three wellbore structures when the wellhead pumping pressure is 50 MPa and the pumping displacement is 5 m³/min The field distribution diagram is shown in Fig. 6. It is found that during the acid fracturing process, the temperature of the tubing string at all levels in the wellbore increases to varying degrees compared

Table 2. Summary of well bore structure and integrated pipe string structure data used

Number	Well type	Well depth [m]	Intermediate casing diameter [mm]	Production casing diameter [mm]	Tubing diameter [mm]	Packer depth [m]
X1	Vertical	4000	381.0	254.0	177.80	2100
X2	Deviated	2500	/	254.0	177.80	2200
X3	Horizontal	3750	342.9	247.65	177.80	1900

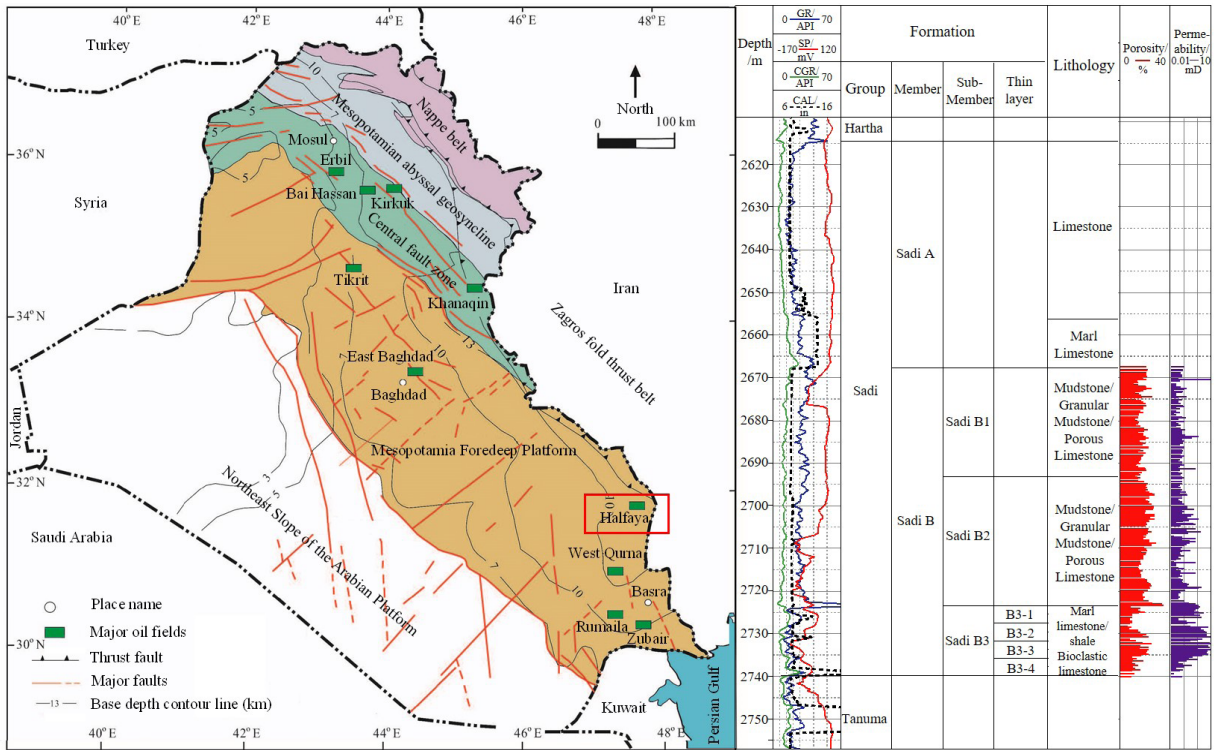


Fig. 5. Sadi formation information comprehensive histogram

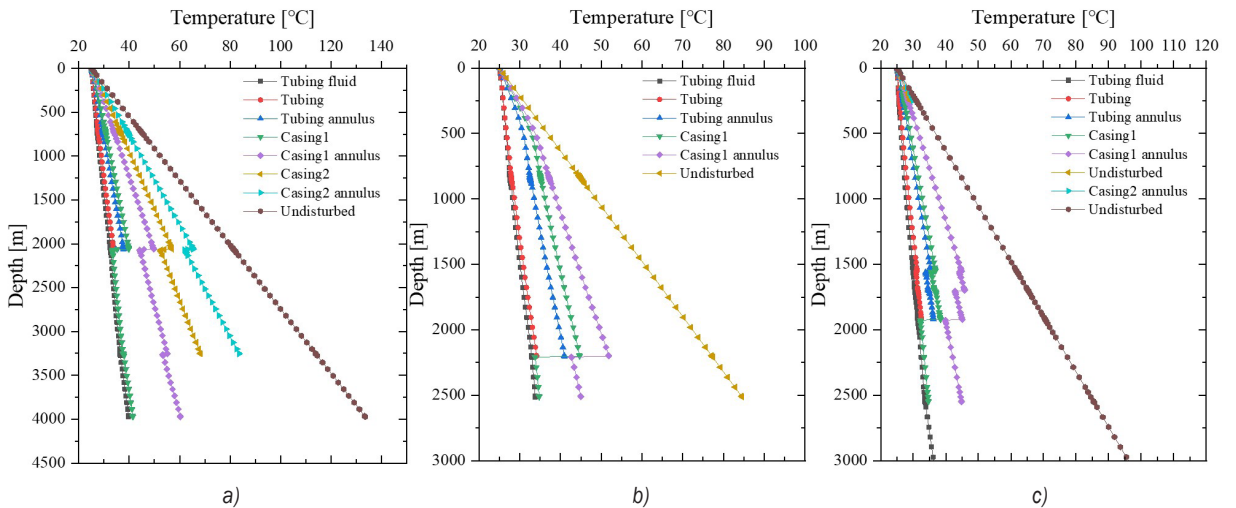


Fig. 6. Temperature distribution curve with depth in wellbore; a) X1 vertical well, b) X2 deviated well, and c) X3 horizontal well

with the wellhead. However, due to the injection of fracturing fluid into the wellhead, the temperature near the oil pipe is lower at the same depth, and the farther layers are closer to the formation temperature. Additionally, due to the role of the integrated string packer, temperature faults occur at the packer, as shown in Table 3.

Table 3. Temperature statistics at the upper and lower packers

Number	Well type	Packer depth [m]	Upper [°C]	Lower [°C]
X1	Vertical	2100	38.5	27.3
X2	Deviated	2200	33.2	26.7
X3	Horizontal	1900	31.9	25.8

2.2 Analysis of Axial Force Calculation Results for Integrated Pipe String

Because the axial force of the integrated pipe column directly determines the safety status of the pipe column during service, attention needs to be paid to it, so the axial force distribution curve of the integrated

string under different displacement and pump pressure conditions is obtained through software simulation calculation, as shown in Fig. 7, it is found that the axial force of the string at the wellhead is axial tension, while the axial compression force is generated at the bottom of the well, and the position where the axial force is 0 appears at the packer. Due

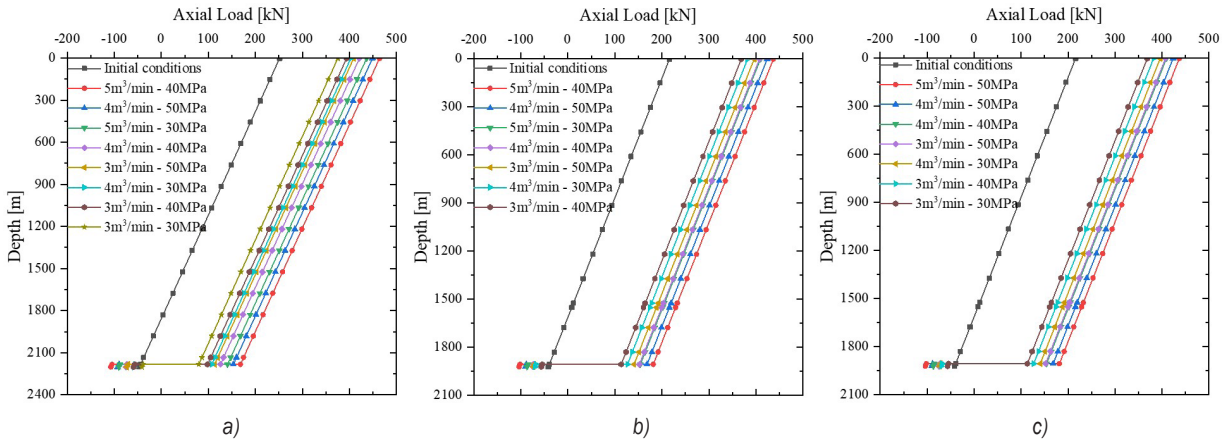


Fig. 7. Distribution curve of axial force in Wellbore with depth; a) X1 vertical well, b) X2 deviated well, c) X3 horizontal well

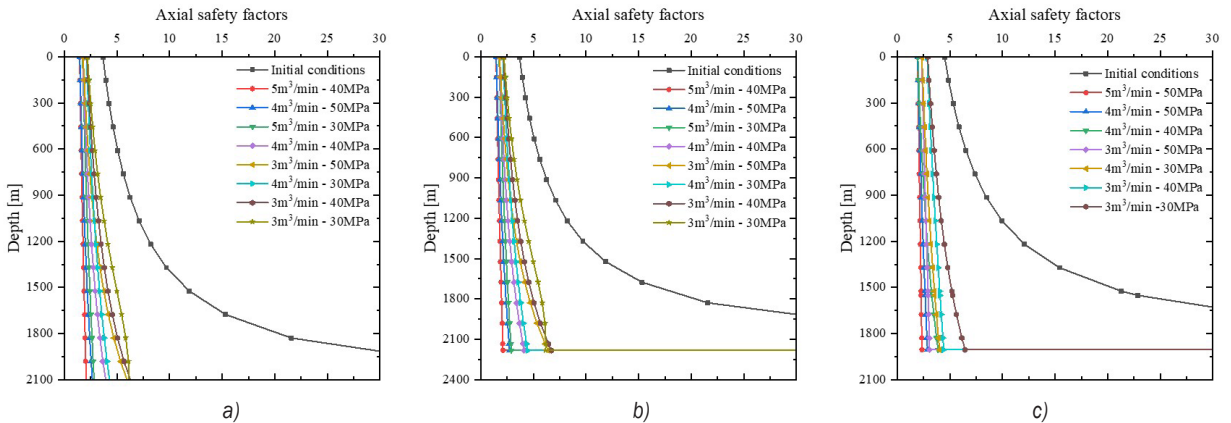


Fig. 8. Distribution curve of axial safety factor in Wellbore with depth; a) X1 vertical well, b) X2 deviated well, c) X3 horizontal well

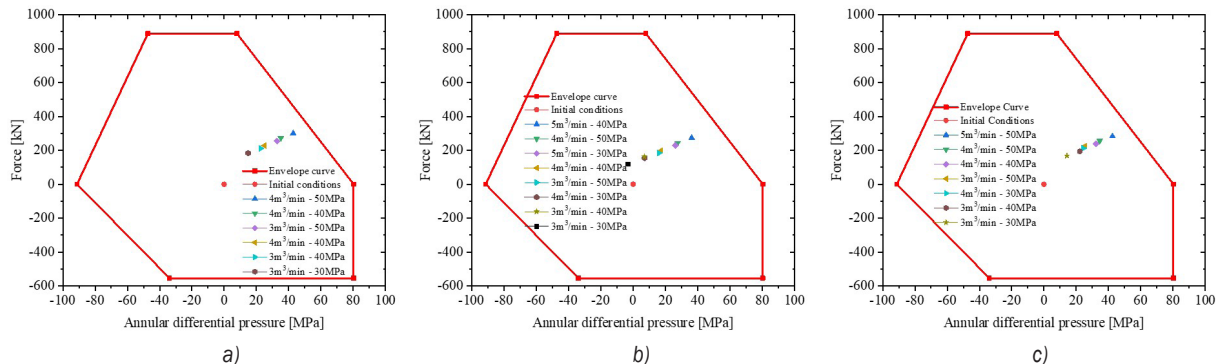


Fig. 9. Load distribution of RTTS packers under different working conditions and well shapes; a) X1 vertical well, b) X2 deviated well, c) X3 horizontal well

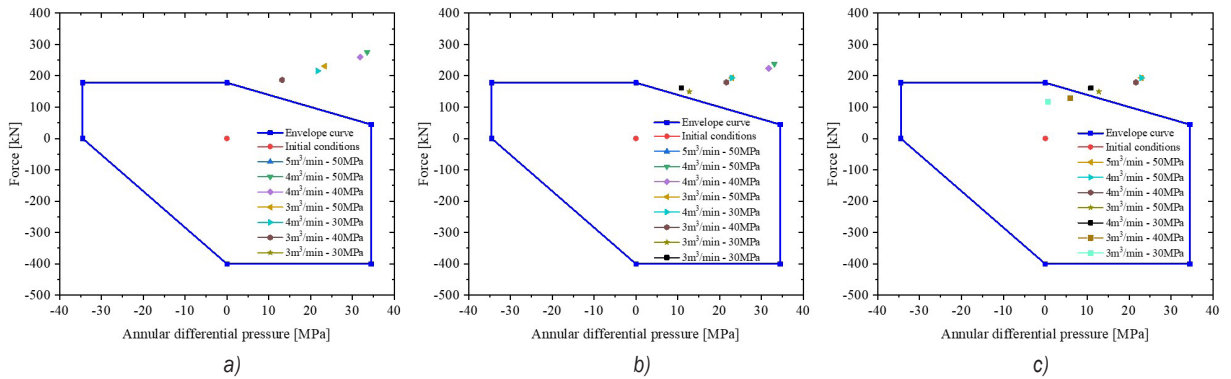


Fig. 10. Load distribution of well completion packers under different working conditions and well shapes; a) X1 vertical well, b) X2 deviated well, c) X3 horizontal well

to the cold contraction of the pipe string during the acid fracturing process, the normal packer prevents the displacement of the string. In order to intuitively judge the safety state of the string, the axial safety factors of each well type are summarized in Fig. 8 It is found that the axial safety factors of all pipe strings are greater than 1, indicating that the pipe strings are in a safe state and there will be no phenomenon of plastic tensile fracture.

Through model calculation, the evaluation diagrams of load and envelope curves of RTTS packer and RH packer are shown in Figs. 9 and 10. It is found that the RTTS packer is applicable in all working conditions, and the RH packer cannot be applied in most cases due to its weak packer capability.

3 STRESS ANALYSIS OF INTEGRATED STRING PACKER

3.1 Establishment of Finite Element Model for RTTS Packer

According to the model established in the second section, the analysis shows that only the RTTS packer is suitable for the use of the integrated string in this oilfield; therefore, based on the actual use of the integrated string structure in an oilfield in Middle East, a static 2D axisymmetric finite element mechanical simulation of the RTTS packer is established using ABAQUS. In the finite element model, the number of finite elements is 17,207, the number of nodes are 18455, including 16,837 quadrilateral finite elements (CAX4R), 370 triangular finite elements (CAX3), the size of the casing finite elements is 10 mm, the size of the centre pipe is 10 mm, and the other components are 1 mm. The model and its finite elements model are shown in Fig. 11. In the figure, the RTTS packer is mainly composed of connectors, rubber ring, spacers,

slip cones, slips, and tubing. When the RTTS packer is in normal operation, pressure is applied downwards from the connectors, and squeezed after the slip pressure cone stretches the slips, it bites on the inner wall of the casing to fix the packer and then continues to exert axial pressure on the joint to squeeze and deform the rubber ring to seal the inner wall of the casing, so that the centre pipe and the annulus between the casing can maintain a certain pressure difference between the upper and lower sides, so as to avoid the temperature effect caused by the temperature decrease during the acid fracturing process, which will cause the axial displacement of the integrated pipe string.

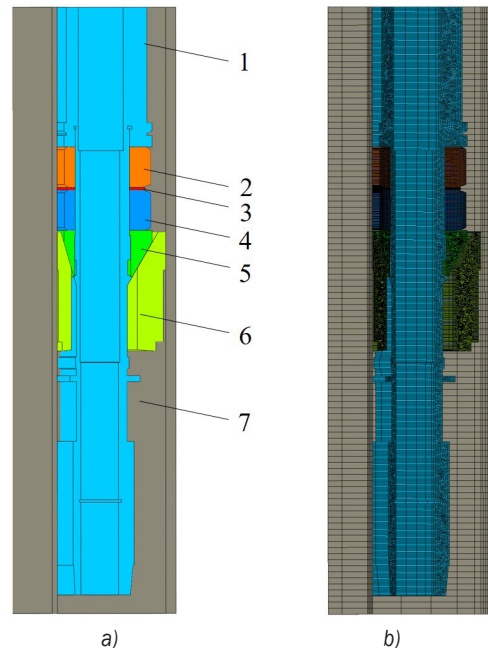


Fig. 11. Finite Element Mechanical Model of RTTS Packer; a) solid model, and b) finite elements model; (1 connector, 2 and 4 rubber ring, 3 spacer ring, 5 slip cone, 6 slip, and 7 casing)

The RTTS packer mainly uses two materials: steel and rubber. The Poisson's ratio of the steel is 0.3, the elastic modulus is 2.1×10^5 MPa, the yield strength is 758.6 MPa, and the tensile strength is 862 MPa. Comprising propylene-polytetrafluoroethylene material, high temperature resistance, high pressure, reliable sealing performance, compressive strength up to 60 MPa, the rubber ring and the end protection ring are vulcanized into one, prevent shoulder protrusions on the rubber ring, improve the pressure resistance of the rubber ring, and are used for the rubber material of the rubber ring Mooney-Rivlin constitutive model, in which parameters $C_{10} = 1.879$ MPa, $C_{01} = 0.038$ MPa, and temperature and axial force data obtained by software simulation are attached to the packer. The force situation of the packer from running into fracturing operation is simplified into four steps: the stage of fixed constraint, the stage of applying gravity, the stage of applying setting force, and the stage of applying internal and external pressure and axial force. The whole load and boundary a summary of the conditions imposed is shown in Fig. 12. In the fixed constraint stage, the slips are in a fixed state during the entire stress process, so fixed constraints are applied to the lower part of the slips, and secondly, in

the gravity application stage, after the slips are fixed, the gravity of the entire string is applied to the packer. Then apply the upper axial force on the joint in the stage of applying the setting force, and finally apply the lower axial force and the internal and external pressure in the model in the stage of applying the internal and external pressure and axial force, which were simulated in Section 2 and are affected by the temperature difference; the applied load is shown in Table 4.

3.2 Finite Element Analysis Results of RTTS Packer

Through the finite element calculation of the established model, the stress distribution image of the three wells under different acid fracturing conditions are shown in Fig. 13.

Analysis of the worst acid fracturing conditions in the field, when the wellhead pressure is 50 MPa and the displacement is 5 m³/min, the maximum stress on the packer does not exceed 400 MPa, which is much smaller than the yield strength of the RTTS packer, indicating that at this time it is in the safe state, the maximum stress value appears in the lower part of the

Table 4. Summary of the stress situation during the setting stage of RTTS packer

Well number	Axial force F1 [kN]	Axial force F2 [kN]	Internal pressure Pin [MPa]	Upper external pressure Pout1 [MPa]	Lower external pressure Pout2 [MPa]
X1	100	84.28	61.98	19.59	61.98
X2	100	106.87	64.18	27.98	64.14
X3	100	103.77	50.38	18.64	50.34

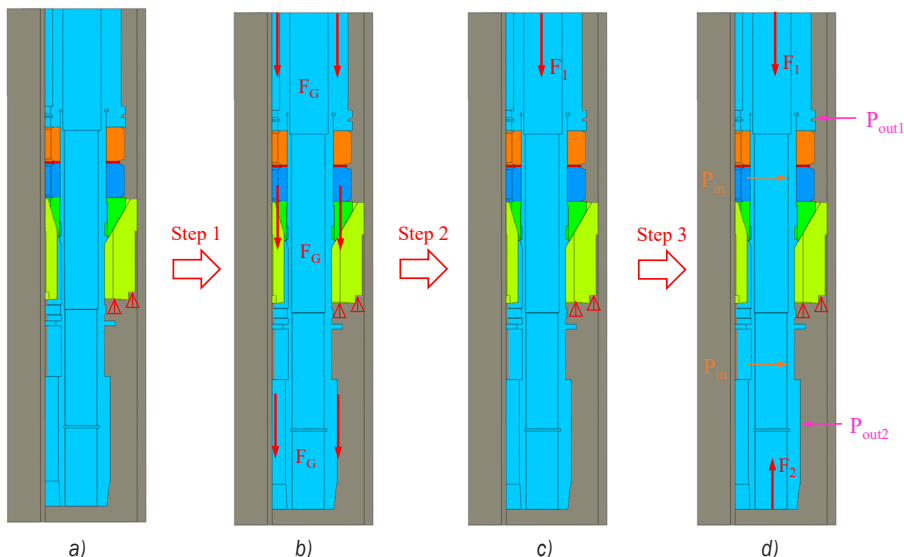


Fig. 12. Schematic diagram of constraints and forces during the setting stage of RTTS packer; a) fixed constraints, b) apply gravity, c) apply sealing force, and d) apply pressure and axial force

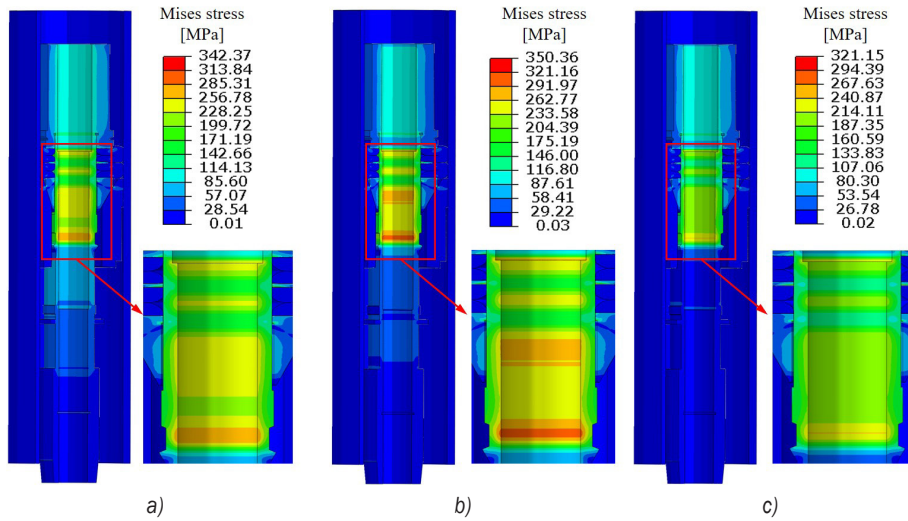


Fig. 13. Stress distribution image of RTTS packer under acid fracturing conditions; a) X1 vertical well, b) X2 deviated well, and c) X3 horizontal well, (1 central tube, 2 rubber ring, 3 slip, and 4 casing)

centre pipe, and the rubber ring is greatly deformed, completely sealing the annulus between the pipe strings, and achieving a complete seal, indicating that the RTTS packer can meet the actual requirements of the site. However, in order to achieve the purpose of eliminating potential safety hazards in actual operation, it is recommended to increase the wall thickness of the lower part of the central tube.

As a key component for sealing in the packer, the rubber ring can be evaluated for its sealing performance using the Mises stress and contact pressure on the rubber ring. Therefore, the Mises

distribution image and contact pressure distribution image were obtained through a finite analysis model, as shown in Figs 14 and 15, respectively. From the Mises distribution image, it is found that in the worst working conditions of each well, the maximum stress on the rubber ring has reached 60 MPa, but the material of the rubber ring is a special type of rubber, it still does not break under the stress state. The reason for the possible failure of the upper rubber ring is the failure of the seal; the contact pressure of the rubber ring in contact with the outer wall is 0 MPa. As shown in Fig. 16, the distribution shows that the maximum

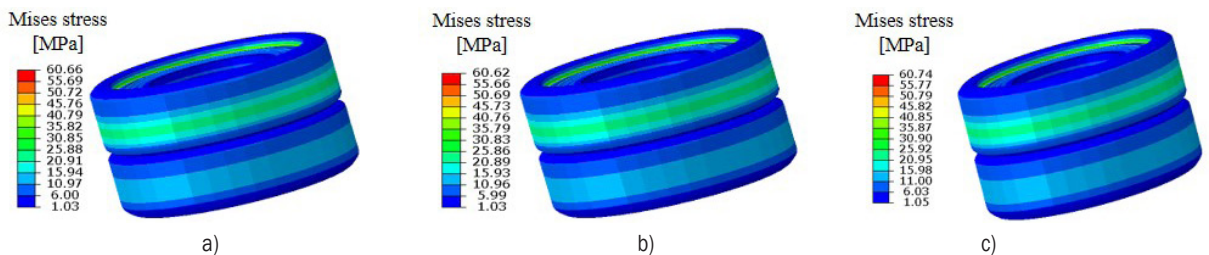


Fig. 14. Mises stress distribution image in RTTS packer rubber ring; a) X1 vertical well, b) X2 deviated well, and c) X3 horizontal well

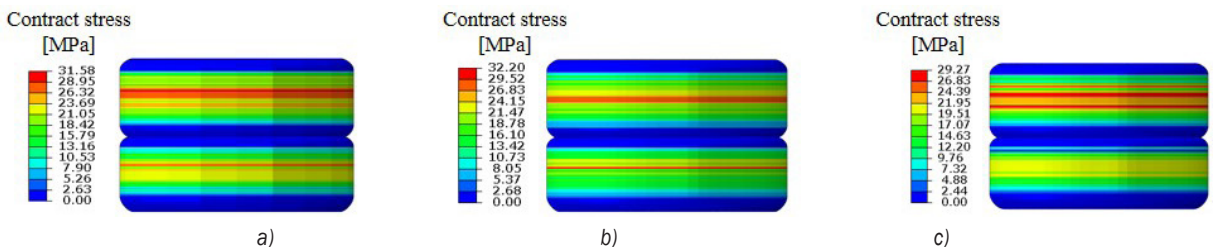


Fig. 15. Contact stress distribution image of RTTS packer rubber ring; a) X1 vertical well, b) X2 deviated well, and c) X3 horizontal well

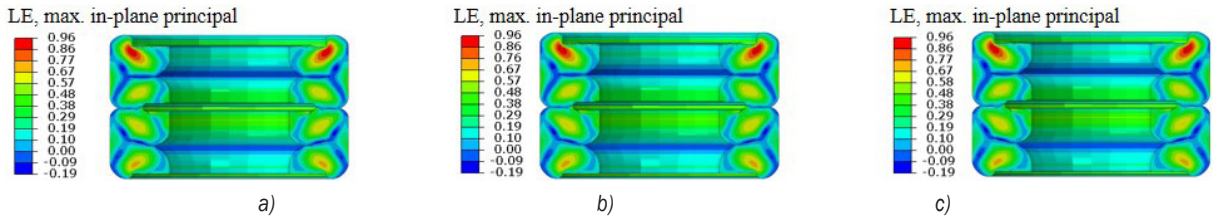


Fig. 16. Strain distribution image of RTTS packer rubber ring; a) X1 vertical well, b) X2 deviated well, and c) X3 horizontal well

principal logarithmic strain of the upper rubber ring is greater than that of the lower rubber ring, but the material of the rubber ring is rubber. In the case of such a large strain, it can still work safely, but the extrusion part of the upper joint can be optimized in the design. The structure makes the deformation of the upper and lower joints similar, unifies the service life of the packer rubber ring, and facilitates the replacement of the rubber ring at the same time.

The contact pressure distribution curve of the contact part between the packer rubber ring and the outer wall casing is extracted, as shown in Fig. 17; the contact pressure on the rubber ring reaches about 30 MPa, indicating that the rubber ring can still maintain good performance under the worst working conditions. The sealing performance is excellent, and the contact pressure of the upper rubber ring is larger than that of the lower rubber ring, but it can fully meet the requirements of the integrated string packer in the oil field.

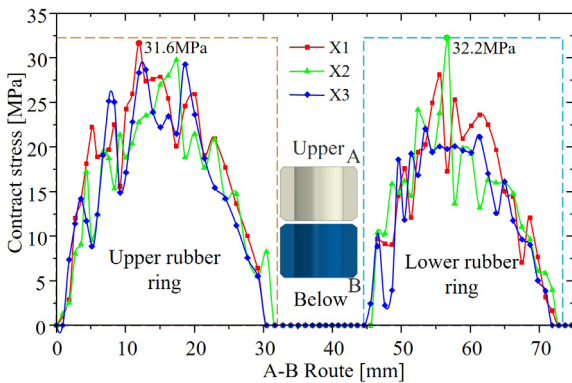


Fig. 17. Contact pressure distribution curve of the contact part of the rubber ring

4 CONCLUSIONS

(1) Based on the dimensions and production data of three different wellbore structures provided on site, a multi-factor analysis model for the wellbore was established. The temperature, axial

force of the tubing, and safety factor distribution of each part of the wellbore were calculated for three different wellbore types in a middle eastern oilfield. The analysed data provides a theoretical basis for on-site well control.

- (2) According to the finite element model of the mechanical distribution of the packer structure during acid fracturing established in this article, this model can simulate the stress distribution of various components in the packer under various working conditions during the acid fracturing process after the packer is set, and then evaluate the adaptability of the packer. It provides a reliable theoretical basis for the safety evaluation of the packer in the safe production of oil and gas fields.
- (3) The three types of wells studied in the article can all meet the needs of safety production using RTTS packers. However, the use of completion packers can lead to insufficient sealing capacity and safety production hazards. Therefore, using RTTS packers in integrated pipe strings is recommended.
- (4) Through a large number of finite element calculations and analyses, the packer can withstand the wellhead displacement of 5 m³/min and wellhead pressure of 50 MPa, which is the worst production condition on site. At this time, the maximum stress of the packer appears on the centre pipe of the packer, so special attention should be paid in the production process, and the contact pressure on the rubber ring reaches 30MPa without sealing contact failure.
- (5) In the process of fracturing bottom layer stimulation, when the normal temperature fracturing fluid injected at the wellhead reaches the target formation, it causes the downhole string to cool down, causing the axial tension of the string to reach 500 kN due to thermal expansion. In order to reduce the axial tension of wellhead equipment and prevent accidents such as wellhead falling, adding expansion joints in the string is recommended.

5 ACKNOWLEDGEMENTS

This work was supported by the Sichuan Province Science and Technology Program (No. 2023NSFSC0427).

6 REFERENCES

- [1] Qi, N., Chen, G.B., Liang, C., Guo, T.K., Liu, G.L., Zhang, K. (2019). Numerical simulation and analysis of the influence of fracture geometry on wormhole propagation in carbonate reservoirs. *Chemical Engineering Science*, vol. 198, no. 1, p. 124-143, DOI:10.1016/j.ces.2018.12.047.
- [2] Zhu, D., Hu, Y., Cui, M., Chen, Y., Liang, C., He, Y., Wang, X., Wang, D. (2019). Feasibility analysis on the pilot test of acid fracturing for carbonate reservoirs in Halfaya Oilfield, Iraq. *Energy Science & Engineering*, vol. 7, no. 3, p. 721-729, DOI:10.1002/ese3.290.
- [3] Al-salali, Y., Al-Bader, H., Duggirala, V., Manimaran, A., Packirisamy, S., Al-Ibrahim, A., Rajkhowa, A. (2013). Challenges in testing and completion of highly sour HPHT reservoir in the State of Kuwait. *SPE Kuwait Oil and Gas Show and Conference*, art. ID 164311, DOI:10.2118/164311-MS.
- [4] Bybee, K. (2006). Continuous improvements in acid fracturing at Lake Maracaibo. *Journal of Petroleum Technology*, vol. 58, no. 7, p. 54-56, DOI:10.2118/0706-0054-JPT.
- [5] Cohen, C.E., Tardy, P.M.J., Lesko, T.M., Lecerf, B.H., Mchawah, A. (2010). Understanding Diversion with a Novel Fiber-Laden Acid System for Matrix Acidizing of Carbonate Formations. *SPE annual technical conference and exhibition*, art. ID 134495, DOI:10.2118/134495-MS.
- [6] Chen, Y., Tan, J., Xiao, G. (2021). Investigation on the depth of slip hanger teeth bite into casing and the mechanical properties of casing under different suspension loads in ultra-deep wells. *Strojniški vestnik-Journal of Mechanical Engineering*, vol. 67, no. 10, p. 516-524, DOI:10.5545/sv-jme.2021.7251.
- [7] Qi, Y., Wu, Z.F., Bai, X.H. (2013). Fracture design optimization of horizontal wells targeting the Chang 6 formation in the Huaqing Oilfield. *SPE Asia Pacific Unconventional Resources Conference and Exhibition*, art. ID 167008, DOI:10.2118/167008-MS.
- [8] Hassani, F., Faisal, N.H., Nish, R., Rothnie, S., Njuguna, J. (2021). The impact of thermal ageing on sealing performance of HNBR packing elements in downhole installations in oilfield wellhead applications. *Journal of Petroleum Science and Engineering*, vol. 208, p. 109200, DOI:10.1016/j.petrol.2021.109200.
- [9] Zhang, J., Xie, J. (2018). Investigation of static and dynamic seal performances of a rubber O-ring. *Journal of Tribology*, vol. 140, no. 4, art. ID O42202, DOI:10.1115/1.4038959.
- [10] Koblar, D., Škofic, J., Boltežar, M. (2014). Evaluation of the young's modulus of rubber-like materials bonded to rigid surfaces with respect to Poisson's ratio. *Strojniški vestnik-Journal of Mechanical Engineering*, vol. 60, no. 7-8, p. 506-511, DOI:10.5545/sv-jme.2013.1510.
- [11] Polonsky, V. L., Tyurin, A. P. (2015). Design of packers for sealing of the inter-tube space in equipment used for recovery of oil and gas. *Chemical and Petroleum Engineering*, vol. 51, no. 1-2, p. 37-40, DOI:10.1007/s10556-015-9994-2.
- [12] Lopez, G. J. N., Amaya, M., Mora, J. H., Agudelo, O. (2010). Integrated sand-production management in a heterogeneous and multilayer mature field with water injection. *SPE Latin America and Caribbean Petroleum Engineering Conference*, art. ID. 139378, DOI:10.2118/139378-MS.
- [13] Liu, Y., Lian, Z.H. (2021). Failure analysis on rubber sealing structure of mandrel hanger and improvement in extreme environments. *Engineering Failure Analysis*, vol. 125, art. ID 105433, DOI:10.1016/j.engfailanal.2021.105433.
- [14] Liu, Y., Qian, L., Xia, C., Zou, J., Lian, Z.H., Yi, X. (2023). Failure analysis and structural optimization of rubber core and support rib of full-size spherical blowout preventer. *Engineering Failure Analysis*, vol. 143, art. ID 106865, DOI:10.1016/j.engfailanal.2022.106865.
- [15] Karadžić, U., Bergant, A., Starinac, D., Božović, B. (2019). Water hammer investigation of the shut-down of a high-head hydropower plant at very high Reynolds number flows. *Strojniški vestnik-Journal of Mechanical Engineering*, vol. 65, no. 7-8, p. 430-440, DOI:10.5545/sv-jme.2019.6092.
- [16] Jin, L., Xue, Z., Wang, Z., Li, R., Liu, J. (2023). Mechanical response of the sealing packer based on two rubber materials at high temperatures. *Polymer Testing*, vol. 124, no. 5, art. ID 108073, DOI:10.1016/j.polymertesting.2023.108073.
- [17] Hu, G. (2018). Study on sealing performance of packing element in permanent packer under complicated conditions. *Southwest Petroleum University*, DOI:10.27420/d.cnki.gxsync.2018.000425. (in Chinese)
- [18] Liu, Y., Qian, L., Zou, J., Xia, C., Lian, Z.H. (2022). Study on failure mechanism and sealing performance optimization of compression packer. *Engineering Failure Analysis*, vol. 136, art. ID 106176, DOI:10.1016/j.engfailanal.2022.106176.
- [19] Mitchell, R. F. (2012). Buckling of tubing inside casing. *SPE Drilling & Completion*, vol. 27, no. 4, p. 486-492, DOI:10.2118/150613-MS.
- [20] Wang, Y.X., Zhou W., Guo R., (2017). shoal facies reservoir characteristics and genesis of mishrif formation in Halfaya oilfield, Iraq. *Journal of Jilin University*, vol. 47, no. 4, p. 1007-1020, DOI:10.13278/j.cnki.jjuese.201704104. (in Chinese)